Korean J. of Chem. Eng., 9(1), 29-36 (1992)

SIMULATION OF SILICON FILM GROWTH BY SILANE DECOMPOSITION IN A MERCURY-SENSITIZED PHOTO-CVD PROCESS

Ju Hyung Lee, Sang Heup Moon* and Shi-Woo Rhee**

Dept. of Chemical Engineering, Seoul National University, Kwanak-ku, Shinlim-dong, San 56-1, Seoul, Korea
**Dept. of Chemical Engineering, Pohang Institute of Science and Technology, P.O. Box 125, Pohang, Korea
(*Received 2 December 1991 • accepted 15 February 1992*)

Abstract—Deposition of silicon film by a mercury-sensitized photo-CVD process has been simulated by numerical solution of governing equations with proper boundary conditions. The results indicate that the film deposition rate is controlled by homogeneous decomposition of the reactant, silane, in the gas phase. The growth rate increases but the film uniformity decreases with the increase of reactant inlet concentration. Increase in the reactant flow rate decreases the deposition rate but gives no effect on the film uniformity. Among process variables, the light intensity and the mercury-saturator temperature are important parameters.

INTRODUCTION

Photo-CVD is a new promising technique for preparation of thin films [1-3], and has many advantages over other CVD methods, particularly in that it proceeds at low-temperatures. Unlike high energy ionized molecules in PECVD (Plasma Enhanced CVD), the dissociated reactants are electrically neutral (or free radicals) and therefore films of good quality can be grown. Since a given molecule absorbs light only at specific wavelengths, the choice of photons from lamps or lasers also allows for a high degree of selectivity and a great control of the deposition process.

Although it has long [4] been known that SiH_4 is decomposed by mercury photo-sensitization, application of this method to microelectronics processing is relatively recent. Lampe and his coworkers [5-7] steadily reported the results of their observations on the photolysis and photo-sensitized decomposition of silane compounds. On the basis of these results, detailed kinetics for mercury-sensitized photo-CVD was proposed by Matsui et al. [8]. Kmisako et al. [9] performed similar work to that of Matsui et al. [8] and obtained informations on the deposition mechanism of a-SiH film.

Despite these works, however, there is no published article which deals with the effect of process variables on the film growth rate and the uniformity, although they are the most required informations in the actual fabrication.

In this work, mercury-sensitized UV-CVD process has been modeled and analyzed mathematically to investigate the effect of process variables on the film growth rate and uniformity.

*To whom correspondence related to this paper should be addressed.

MODEL FORMULATION

A schematic diagram of a typical photo-CVD apparatus is shown in Fig. 1. Presently, most photo-CVD methods are used for growing of hydrogenated amorphous silicon films [10]. Reactant gases, silane-hydrogen or silane-helium mixtures, are introduced into the reaction chamber after passing through a mercury saturator where the amount of mercury vapor is controlled thermally. UV light with the wavenumber ranging between 185 and 250 nm is emitted from a low-pressure mercury lamp to dissociate the reactant gas molecules.

The photo-CVD reactor is usually operated under the conditions of low pressures (near 1 Torr), low substrate temperatures (lower than 400℃) and with high silane concentrations. Typical operating conditions of the reactor are shown in Table 1.

1. Transport Equations

With the assumptions of steady-state operation and

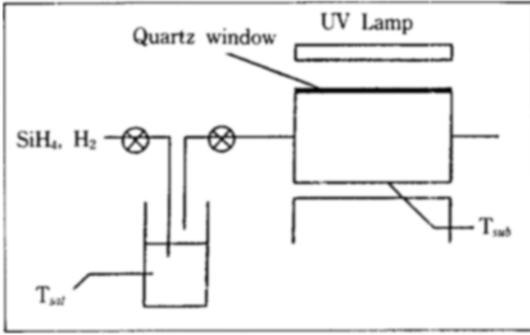

Fig. 1. Schematic diagram of photo-CVD reactor used in modeling.

Table 1. Typical operating conditions in photo-CVD

Temperature	Inlet	: 298 K
	Saturator	: 353 K
	Wall	: 523 K
	Substrate	: 523 K
Pressure		1 Torr
Total flow rate		50 sccm
Inlet SiH_4 Fraction		: 0.8
H_2 Fraction		: 0.2
Production rate		: 10^{-8} g/cm$^3\cdot$s
Reactor dimension		: 3 (height)×14 (length) cm^2

negligible influence of natural convection and thermal diffusion, the transport equations for a two-dimensional photo-CVD process are simplified as follows [11]. Similar assumptions have been made for a thermal LPCVD process in our previous study [12].

Continuity

$$\frac{\partial}{\partial x}(\rho v_x)+\frac{\partial}{\partial y}(\rho v_y)=0 \tag{1}$$

Momentum

$$\frac{\partial}{\partial x}(\rho v_x^2)+\frac{\partial}{\partial y}(\rho v_x v_y)=-\frac{\partial P}{\partial x}+\frac{\partial}{\partial x}\left(\mu\frac{\partial v_x}{\partial x}\right)+\frac{\partial}{\partial y}\left(\mu\frac{\partial v_x}{\partial y}\right)+\rho g_x$$

$$\frac{\partial}{\partial x}(\rho v_x v_y)+\frac{\partial}{\partial y}(\rho v_y^2)=-\frac{\partial P}{\partial y}+\frac{\partial}{\partial x}\left(\mu\frac{\partial v_y}{\partial x}\right)+\frac{\partial}{\partial y}\left(\mu\frac{\partial v_y}{\partial y}\right)+\rho g_y \tag{2}$$

Energy

$$\frac{\partial}{\partial x}(\rho C_p v_x T)+\frac{\partial}{\partial y}(\rho C_p v_y T)=\frac{\partial}{\partial x}\left(\lambda\frac{\partial T}{\partial x}\right)+\frac{\partial}{\partial y}\left(\lambda\frac{\partial T}{\partial y}\right) \tag{3}$$

Mass

$$\frac{\partial}{\partial x}(\rho v_x w_i)+\frac{\partial}{\partial y}(\rho v_y w_i)=\frac{\partial}{\partial x}\left(D_i\frac{\partial w_i}{\partial x}\right)+\frac{\partial}{\partial y}\left(D_i\frac{\partial w_i}{\partial y}\right)+r_i \tag{4}$$

where ρ, μ, C_p, and λ are density, viscosity, heat capacity and thermal conductivity calculated by considering all the species in the reactor. D_i, w_i, and r_i are diffusivity, mass fraction and production rate of the component i (SiH_4, SiH_3, SiH_2, H_2, H, Hg, Hg*, HgH). The total number of differential equation is 12.

2. Kinetic Expression

Since photo-CVD process is operated at low temperatures and pressures, a detailed knowledge of the reaction kinetics is essential for interpreting the phenomena in the reactor. When silane is used as a source gas for deposition, a small quantity of mercury has to be added to the gas mixture because silane does not dissociate in the range of UV wavelength emitted from the low-pressure mercury lamp. The addition of mercury makes it much more difficult to clarify the mechanism of decomposition reaction.

Matsui et al. [8], based on the results previously reported, proposed 17 elementary reaction steps for homogeneous decomposition of silane which are analogous to those proposed by Coltrin et al. [13] in thermal CVD process. Among the species included in their reaction steps, however, there are some insignificant species. The quantities of high order silanes such as Si_2H_6, Si_3H_8 and Si_4H_{10} are found to be small when SiH_4 is used as a source gas [14]. Also, high order free radicals (e.g. Si_2H_5, Si_2H_4) scarcely contribute to film formation compared to radicals such as SiH_2 and SiH_3.

Based on the above consideration, the reactions selected from the steps proposed by Matsui et al. [8] are summarized in Table 2. The last reaction in Table 2 has been included considering the phenomenon of silane saturation which is reported in the other literature [15].

Major differences in the kinetic expressions between the conventional thermal-CVD [12,13] and the UV-CVD considered in this study are that 1) silane decomposition proceeds at relatively low temperatures and 2) mercury vapor has been included in the reactant mixture as a 'UV-sensitizer'. Role of mercury vapor as a sensitizer is to absorb the UV light, be excited to an unstable state, and eventually transfer the excess energy to SiH_4 and H_2 so that the reactants

Table 2. Selected homogeneous reaction kinetics* for photo-CVD

Reaction	$A\times10^{-13}$	E/R
$Hg+h\nu\rightarrow Hg^*$		
$H_2+Hg^*\rightarrow H+HgH$	7.7	0
$H_2+Hg^*\rightarrow H+H+Hg$	3.3	0
$SiH_4+Hg^*\rightarrow SiH_3+H+Hg$	5.1	0
$SiH_4+H\rightarrow SiH_3+H_2$	1.7	1250
$SiH_3+SiH_3\rightarrow SiH_4+SiH_2$	1.8	0
$HgH+SiH_3\rightarrow Hg+SiH_4$	300	0

*Rate constant is given in the form $k=A\cdot\exp(-E/RT)$, where A and E are in the units $cm^3\cdot mol^{-1}\cdot s^{-1}$ and cal/mol, respectively.

Table 3. Sticking coefficients for the species in photo-CVD

Species	β(i)
H_2	0.0
H	1.0
SiH_4	0.0
SiH_3	0.1
SiH_2	1.0
Si_2H_6	0.0
Hg	0.0
Hg^*	1.0
HgH	1.0

undergo successive decomposition reactions.

The photochemical reaction to produce the excited mercury species proceeds almost spontaneously by UV irradiation, activation energy of the reaction being negligible as specified in Table 2. The rate of the mercury excitation, or the production rate, is therefore proportional to the intensity of UV absorption by the mercury vapor.

$$r_{Hg^*}=\Omega\cdot I_{abs} \tag{5}$$

The quantum yield, Ω, is defined as the number of reactant molecules excited for each photon of light absorbed. The UV intensity from the light source, I_0, is usually constant and pre-determined by the lamp characteristics, but the intensity of radiation absorbed by the reactant species, I_{abs}, changes according to the Beer-Lambert law.

$$\frac{I_{abs}}{I}=1-\exp(-udc) \tag{6}$$

Here, u is the molar extinction coefficient, d is the depth of absorber through which the light beam has passed, and C is the absorber concentration. When the magnitude of udc is much smaller than 1, above equation may be approximated as follows.

$$\frac{I_{abs}}{I_0}=udc \tag{7}$$

Combining equations (5) and (7), we get the final expression for the rate of mercury excitation.

$$r_{Hg^*}=\Omega\cdot u\cdot d\cdot C_{Hg}\cdot I_0 \tag{8}$$

The constants, Ω, u, and d may be combined together into a new parameter, k_{ht}, and then the final rate equation is given below.

$$r_{Hg^*}=k_{ht}\cdot C_{Hg}\cdot I_0 \tag{9}$$

It should be noticed in equation (9) that the rate of mercury excitation, or the production rate, is proportional to the concentration of the mercury vapor as well as to the light intensity from the UV lamp.

3. Boundary Conditions and Deposition Rate

Boundary conditions for the governing equations are given below.

$$\begin{cases} \text{At } x=0 & : T=T_{inlet},\ C=C_{inlet},\ v_x=v_{inlet},\ v_y=0 \\ \text{At } x=x_L & : \partial\phi/\partial y=0\ (\phi=T,\ C,\ v_x),\ v_y=0 \\ \text{At } y=0 & : T=T_{sub},\ v_x=v_y=0 \\ \text{At } y=h & : T=T_{wall},\ v_x=v_y=0 \end{cases}$$

The four conditions refer to the conditions of inlet, outlet, substrate, and wall of the reactor, respectively. The condition that the concentration of free radical on the wafer surface is zero, which is usually assumed in thermal CVD, can not be used in photo-CVD because in the latter case the surface temperature is low and therefore the assumption of rapid disappearance of free radicals on the wafer surface is no longer valid. Instead, Nishida et al. [10] have suggested that the following surface reactions should be considered.

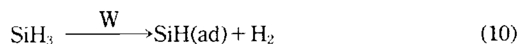

$$SiH_3 \xrightarrow{W} SiH(ad)+H_2 \tag{10}$$

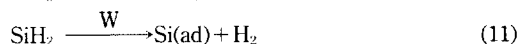

$$SiH_2 \xrightarrow{W} Si(ad)+H_2 \tag{11}$$

Here, 'W' above the arrow indicates that the reaction occurs on the surface and the species with '(ad)' are adsorbed on the surface. Equation (10) indicates that SiH_3 is decomposed incompletely to produce SiH(ad), which contributes to the amount of hydrogen contained in the silicon film.

Since the surface reaction kinetics is not known, the reaction rate of component i, $r_{i,surf}$, on the surface has been estimated from that only a fraction of component i colliding with the surface undergoes the reaction.

Table 4. Important dimensionless variables

Re	Reynolds No.	$D v \rho/\mu$	0.02-0.05
Pe_t	Thermal Peclet No.	$D v/\alpha$	0.01-0.05
Pe_m	Mass Peclet No.	$D v/D_i$	0.01-0.03
Ra	Rayleigh No.	$\beta g C_p \rho^2 h^3 \Delta T/k\mu$	0.0001-0.001
Gr	Grashof No.	$\beta g \rho^2 h^3 \Delta T/\mu^2$	0.001-0.01
Ri	Richardson No.	$\beta g h \Delta T/v^2$	0.01-0.1

$$r_{i,surf} = \beta(i) \cdot Z_{i,surf} \tag{12}$$

Collision frequency of component i with the surface, $Z_{i,surf}$, is derived from the kinetic theory as follows [16].

$$Z_{i,surf} = (RT/2\pi M_i)^{1/2} \cdot C_i \tag{13}$$

Here, M_i and C_i represent molecular weight and molar concentration of component i, respectively. $\beta(i)$, sticking coefficient for component i, represents different strengths of the adsorbed species [17]. In Table 3 are shown the sticking coefficients of various components produced in the photo-CVD process.

Employing the above surface reaction, we may derive the surface boundary condition by equating the flux of diffusion from the bulk with the rate of surface reaction on the wafer.

$$\beta(i) \cdot (RT/2\pi M_i)^{1/2} \cdot C_i = D_i \cdot \frac{\partial C_i}{\partial y} \tag{14}$$

For the other non-consumed species, such as SiH_3, Hg or Hg*, no such equations have been used. Finally, the film growth rate, G, is determined from the total flux of SiH_3 and SiH_2 to the wafer surface.

$$G = 6.00 \cdot 10^5 \cdot \frac{M_{Si}}{\gamma} \cdot \left(D_{SiH_2} \frac{\partial C_{SiH_2}}{\partial y} + D_{SiH_3} \frac{\partial C_{SiH_3}}{\partial y} \right) \tag{15}$$

M_{Si} is the atomic weight of silicon (28.09 g/g-atom), and γ is the density of silicon film (2.33 g/cm^3). C_{SiH_2} and y are in units of gmol/cm^3 and cm.

NUMERICAL COMPUTATION

Numerical computation method used in this study is the same as used in our previous report [12]. That is, a generalized finite difference computer program [18] has been used to solve the coupled model equations for reaction and transport phenomena. The second order parabolic forms of the partial differential equations have been reduced to six-point, finite difference forms, and then solved with TDMA (Tri-Diagonal Matrix Algorithm) [19] by marching integration through the finite difference grid of 21×17 points.

SIMPLE(Semi-Implicit Method for Pressure Linked Equations) algorithm [19] and upwind scheme have been adopted for correct solution and program stability. Typical computational run has required 12 hours using a personal computer of 386-SX.

RESULTS AND DISCUSSION

A typical set of operating conditions used in photo-CVD is listed in Table 1. As explained in section 2-2, the production rate refers to the rate at which the mercury atoms are excited by UV light, and its magnitude has been determined after several computer trial runs by the following procedures. The concentration ratio of nonactivated mercury ($^1S_0$) to excited mercury ($^3P_1$) has been adjusted by varying the 'production rate' so that it has the same ratio as reported in the literature [17]. The dimensionless variables corresponding to the process conditions in Table 1 are listed in Table 4.

1. Typical Results

Fig. 2 shows a schematic view of the velocity field obtained for the operating conditions of Table 1. The flow is fully-developed soon after it enters the reactor. Temperature field in the reactor is given in Fig. 3. It shows that the reactant is heated slowly as the temperature difference between the wall and the inlet reactant is relatively small.

Distribution of the SiH_4 concentration is shown in Fig. 4. The iso-concentration line is almost vertical to the flow direction since the dissociation of SiH_4 is small (less than 10%). The iso-concentration profile of SiH_2 (Fig. 5) shows a similar shape to that of SiH_4 with small variation along the y direction. This is because the reaction of SiH_2 production occurs very rapidly with no dependence on the temperature field (see Table 2). The SiH_3-concentration profile (Fig. 6), however, is much different from the profile of SiH_2. Reaction steps in Table 2 indicate that SiH_3 is produced by thermal activation as well as by instantaneous reaction with the photon-excited mercury.

The deposition rate is small because the iso-concentration lines of SiH_3 and SiH_2 which determine the deposition rate touch the wall almost at a right angle.

2. Effect of Process Variables

2-1. Reactant Flow Rate

In Fig. 7, the deposition rates along the reactor position have been plotted for various flow rates and it is assumed that wafers are loaded at the middle part of the reactor. Results to be noted are that the deposition rate decreases with increasing flow rate but the film thickness uniformity is not influenced by the flow rate.

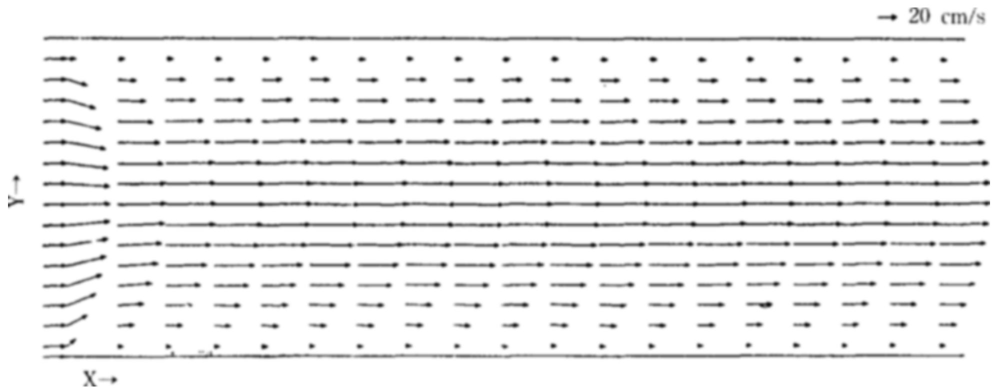

Fig. 2. Typical shape of velocity field (operating conditions in Table 1).

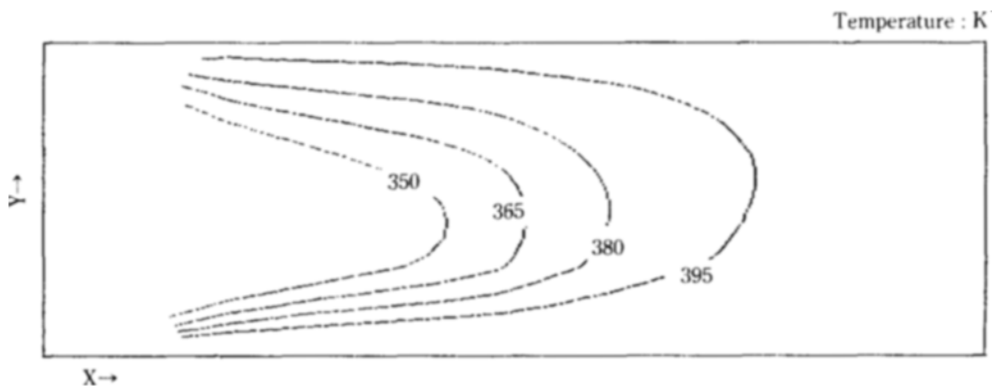

Fig. 3. Typical shape of temperature distribution (operating conditions in Table 1).

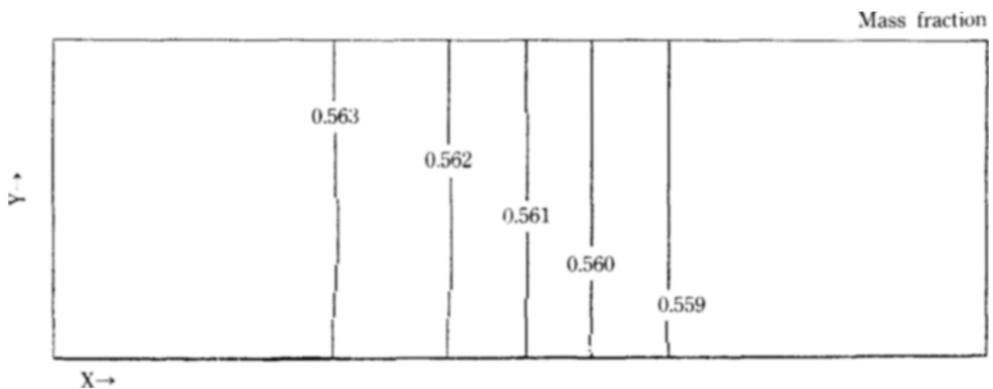

Fig. 4. Typical shape of SiH_4 concentration profile (operating conditions in Table 1).

This result, which is different from the trend observed in thermal LPCVD [12], arises from that the deposition rate in photo-CVD is limited by the temperature-independent decomposition step. The advantage of fast mass transfer with increased flow rate is surpassed by the negative effect of reduced retention time of the deposition precursors in the reactor.

2-2. Inlet Concentration

Variation of the deposition rate with axial positions for several inlet concentrations of SiH_4 is given in Fig. 8. As the inlet concentration increases, the growth rate not only increases but also varies greatly along the reactor position. This is because SiH_4 decomposition is enhanced when the inlet concentration is high. The explanation is supported by the fact that the film uniformity degrades more significantly at the reactor out-

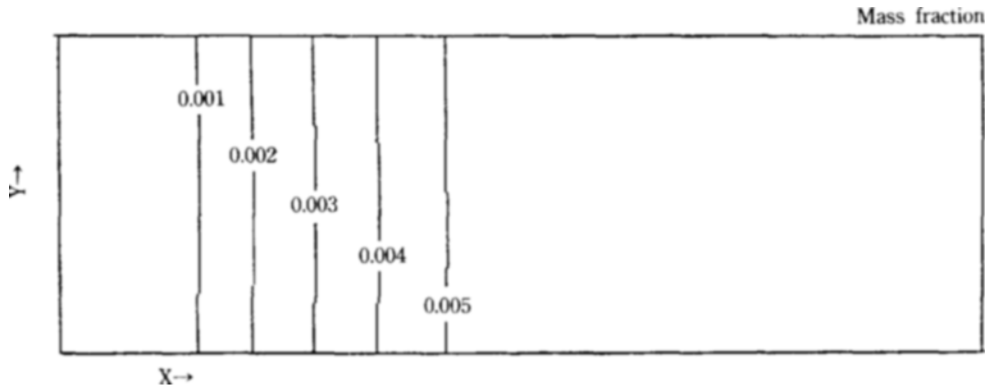

Fig. 5. Typical shape of SiH_2 concentration profile (operating conditions in Table 1).

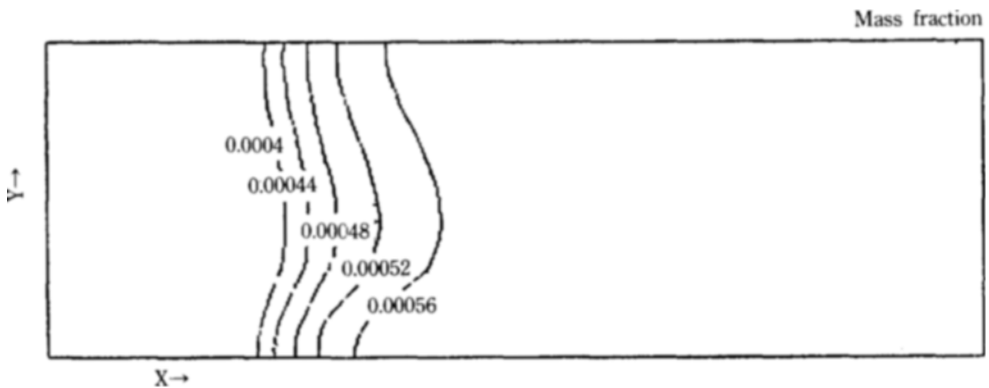

Fig. 6. Typical shape of SiH_3 concentration profile (operating conditions in Table 1).

let than at the inlet when the reactant concentration is gradually lowered.

2-3. Total Pressure

Fig. 9 shows the dependency of the deposition rate and the film uniformity on the total pressure. The growth rate decreases at low pressures due to reduced reactant concentrations, but the film uniformity slightly increases as the pressure decreases. The result is very much different from that in thermal-LPCVD [12], particularly in that the growth rate is less dependent on the mass transfer rate in photo-CVD process.

3. Effect of Optical Parameters

As described in section 2-2, one of the major differences between the conventional thermal CVD and the photo-CVD in this study is that mercury has been used as a UV-sensitizer so that the photochemical reaction is initiated by optical excitation of the mercury vapor. The rate of mercury excitation, i.e., the production rate, is proportional to the lamp intensity and the mercury concentration as derived earlier.

$$r_{Hg^*} = k_{hr} \cdot C_{Hg} \cdot I_0 \quad (16)$$

In this study, we have varied the intensity of the UV lamp and the mercury concentration in proper ranges so that we may compare the relative importance of these variables with that of other process variables such as reactant concentration and total pressure. The intensity of the UV lamp has been decreased to half of the typical condition of Table 1. In the actual experiments, a low-pressure mercury lamp is used for the UV irradiation, and its light intensity changes significantly depending on the mercury pressure in the lamp tube, UV-transparency of the lamp and the window materials, and the distance between the lamp and the CVD reactor [20].

The mercury concentration in the reactant stream is controlled by the temperature of the mercury saturator installed in the CVD system as in Fig. 1. The following thermodynamic correlation exists between the saturator temperature, T_{sat}(K), and the mercury vapor pressure, P_{Hg}(Torr).

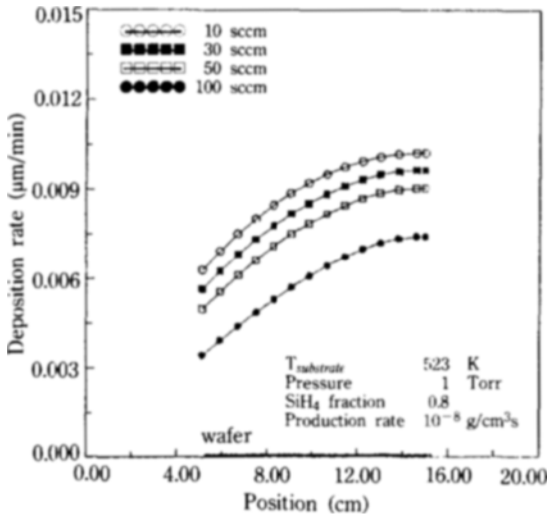

Fig. 7. Deposition rate with position for various flow rate.

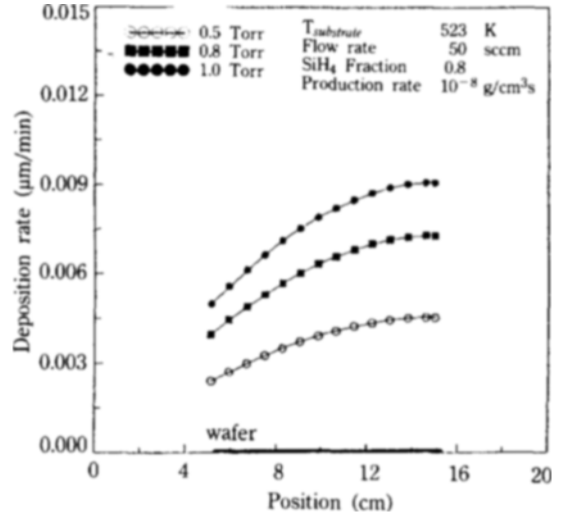

Fig. 9. Deposition rate with position for various total pressure.

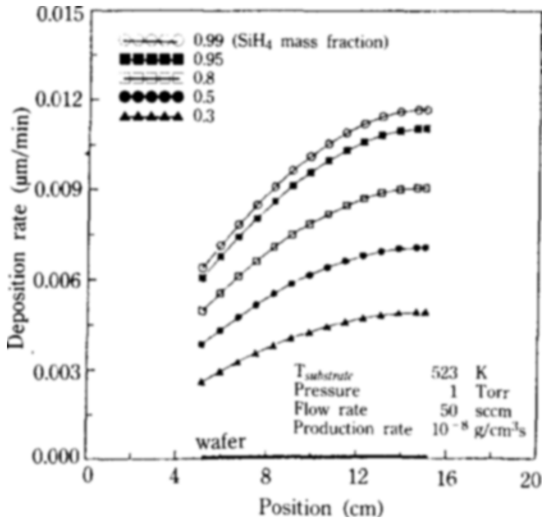

Fig. 8. Deposition rate with position for various inlet concentration of SiH_4.

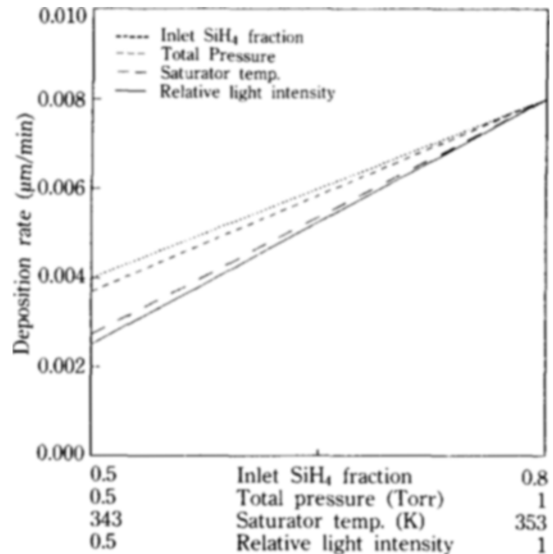

Fig. 10. Dependency of growth rate on process variables.

$$\ln P_{Hg} = 18.6 - \frac{7432.9}{T_{sat}} \qquad (17)$$

In this study, the saturator temperature has been varied between 343 K and 353 K so that the mercury vapor pressure changes between 0.048 Torr and 0.089 Torr, i.e., by about two fold.

Since the film growth rates vary with the axial position in the reactor, the rates under different conditions of the variables have been obtained at the center position of the wafer and the results have been compared in Fig. 10. In the figure, X-axis has been normalized for the variables considered and the actual ranges are given under the axis.

Since the magnitude of each variable is different from each other, it may not be proper to discuss the relative importance of the variables based on the absolute scale. However, within the practical range of the CVD process conditions considered in this study, it appears that the optical parameters such as the UV-lamp intensity and the mercury-saturator temperature make more significant influence on the deposition rate than other variables such as the SiH_4 concentration and the total pressure which are usua-

lly important in thermal CVD processes.

CONCLUSIONS

Dependency of the silicon-film growth rate and the film uniformity on process variables of mercury-sensitized photo-CVD has been studied by computer simulation, and the following conclusions have been obtained.

(1) The deposition rate increases with the reactant inlet concentration, but the film uniformity decreases at high inlet concentrations.

(2) High reactant flow rates offer a negative effect on the deposition rate and no effect on the film uniformity, which is different from the trend observed in thermal CVD.

(3) UV intensity and the mercury-saturator temperature are important parameters to determine the film deposition rate.

ACKNOWLEDGEMENT

This work was supported by Korea Research Foundation, 1991.

NOMENCLATURE

C : concentration
C_p : heat capacity
d : depth of light absorber
D : diffusivity
G : growth rate
g : gravity acceleration
h : reactor height
I : light intensity
k : reaction rate constant
L : reactor length
M : atomic or molecular weight
$r_{i,surf}$: reaction rate of component i on the surface
R : gas constant
T : temperature
u : molar extinction coefficient
v : velocity
w : weight fraction
X : lingitudal position
Y : vertical position
$Z_{i,surf}$: collision frequency of component i on the surface
β : sticking coefficient
γ : density of silicon film
λ : thermal conductivity
μ : viscosity
ρ : density
Ω : quantum yield

REFERENCES

1. Kenne, J., Yamada, A., Konagai, M. and Takahashi, K.: *Jpn. J. Appl. Phys.*, **24**, 997 (1985).
2. Tarui, Y., Hidaka, J. and Aota, K.: *Jpn. J. Appl. Phys.*, **23**, L827 (1984).
3. Toyama, M., Itoh, H. and Moriya, T.: *Jpn. J. Appl. Phys.*, **25**, 679 (1986).
4. Emeleus, H. J. and Stewart, K.: *Trans. Faraday Soc.*, **32**, 1577 (1936).
5. Kamaratos, E. and Lampe, F. W.: *J. Phys. Chem.*, **74**, 2267 (1970).
6. Austin, E. R. and Lampe, F. W.: *J. Phys. Chem.*, **81**, 1134 (1977).
7. Perkins, G. G. A. and Lampe, F. W.: *J. Am. Chem. Soc.*, **102**, 3764 (1980).
8. Matsui, Y., Yuuki, A., Morita, N. and Tachibana, K.: *Jpn. J. Appl. Phys.*, **26**, 1575 (1987).
9. Kmisako, K., Imai, T. and Tarui, Y.: *Jpn. J. Appl. Phys.*, **27**, 1092 (1988).
10. Nishida, S., Tasaki, H., Konagai, M. and Takahashi, K.: *J. Appl. Phys.*, **58**(4), 1427 (1985).
11. Bird, R. B., Stewart, W. E. and Light, E. N.: "Transport Phenomena", John Wiley and Sons Inc., New York (1960).
12. Lee, J. H., Moon, S. H. and Rhee, S. W.: Submitted to Korean J. of Chem. Eng. (1991).
13. Coltrin, M. E., Lee, R. J. and Miller, J. A.: *J. Electrochem. Soc.*, **131**, 425 (1984).
14. Niki, H. and Mains, G. J.: *J. Phys. Chem.*, **68**, 304 (1964).
15. Tachibana, K., Harima, H., Matsui, Y., Yuki, A., Morita, N. and Urano, Y.: *J. Phys. D(Appl. Phys.)*, **20**, 28 (1987).
16. Tompkins, F. C.: "Chemisorption of Gases on Metals", Academic Press, London (1978).
17. Perrin, J. and Broekhuizen, T.: *Appl. Phys. Lett.*, **50**, 433 (1987).
18. Pun, W. M. and Spalding, D. B.: "A General Computer Program for Two-Dimensional Elliptic Flows", Imperial College of Science and Technology, London (1977).
19. Patankar, S. V.: "Numerical Heat Transfer and Fluid Flow", Hemisphere Pub. Corporation, Washington (1980).
20. Abber, R. L.: p. 270 in "Handbook of Thin Film Deposition Processes and Techniques (ed. Schuegraf, K. K.)", Noyes Publications, Park Ridge, NJ (1988).